




Review

# Recent Developments in Prosthesis Sensors, Texture Recognition, and Sensory Stimulation for Upper Limb Prostheses

ANDREW MASTELLER,<sup>1</sup> SRIRAMANA SANKAR,<sup>1</sup> HAN BIEHN KIM,<sup>1</sup>  
KEQIN DING,<sup>1</sup> XIAOGANG LIU,<sup>2,3</sup> and ANGELO H. ALL<sup>4</sup> 

<sup>1</sup>Department of Biomedical Engineering, School of Medicine, Johns Hopkins University, Traylor Building, 720 Rutland Ave, Baltimore, MD 21205, USA; <sup>2</sup>Department of Chemistry, Faculty of Science, National University of Singapore, Building 3 Science Drive 3, 117543 Singapore, Singapore; <sup>3</sup>The N. 1 Institute for Health, National University of Singapore, Singapore, Singapore; and <sup>4</sup>Department of Chemistry, Faculty of Science, Hong Kong Baptist University, # 844, RRS Building, Ho Sin Hang Campus, Hong Kong, Hong Kong

(Received 4 February 2020; accepted 22 October 2020; published online 2 November 2020)

Associate Editor Xiaoxiang Zheng oversaw the review of this article.

**Abstract**—Current developments being made in upper limb prostheses are focused on replacing lost sensory information to the amputees. Providing sensory stimulation from the prosthesis can directly improve control over the prosthetic and provide a sense of body ownership. The focus of this review article is on recent developments while including foundational knowledge for some of the critical concepts in neural prostheses. Reported concepts follow the flow of information from sensors to signal processing, with emphasis on texture recognition, and then to sensory stimulation strategies that reestablish the lost sensory feedback loop. Prosthetic sensors are used to detect the physical environment, converting pressure, force, and position into electrical signals. The electrical signals can then be processed in an effort to identify the surrounding environment using distinctive characteristics such as stiffness and texture. In order for the amputee to use this information in a natural manner, there must be real-time sensory stimulation, perception, and motor control of the prosthesis. Although truly complete sensory replacement has not yet been realized, some basic percepts can be partially restored, allowing progress towards a more realistic prosthesis with natural sensations.

**Keywords**—Nerve electrodes, Sensory feedback, Biomimetic, Noninvasive stimulation, Embodiment, Phantom limb stimulation.

---

Address correspondence to Xiaogang Liu, Department of Chemistry, Faculty of Science, National University of Singapore, Building 3 Science Drive 3, 117543 Singapore, Singapore. Electronic mail: xiaogangliu@nus.edu.sg. Angelo H. All, Department of Chemistry, Faculty of Science, Hong Kong Baptist University, # 844, RRS Building, Ho Sin Hang Campus, Hong Kong, Hong Kong. Electronic mail: angelo@hkbu.edu.hk

Andrew Masteller, Sriramana Sankar, Han Biehn Kim, Keqin Ding contributed equally.

## INTRODUCTION

The parallel advances across neuroscience, neuro-engineering, electronics, and robotics in recent years have led to the development of advanced prostheses. Nevertheless, real-time, accurate, and reliable control of robotic prostheses remains to be effectively achieved.<sup>67</sup> It has been estimated that 40% to 60% of amputees reject the use of their new prostheses, most often due to the lack of fine, precise motor control and unnatural feelings and perceptions.<sup>5,53</sup> There is still an unmet need to develop more realistic and sophisticated sensory feedback systems in order to provide a sense of embodiment or body ownership of these prostheses, which is one of the main focuses of scientists presently.

The natural sensory feedback loop is an intuitive process for healthy individuals. As afferent fibers are stimulated in response to grasping objects or through dexterous movements, an efferent motor response is used to adjust hand movements as needed. Amputees with conventional prostheses lose the ability to feel when or how an object is being grasped and thus cannot adequately modulate their prosthetic hand movements based on natural sensory stimulation. Replacement of this crucial loop starts with sensors that can detect various stimuli from the surrounding environment and physical world. From the use of basic piezoresistive elements to advanced biomimetic implementations, scientists have been exploring how to best mimic and replace subdermal receptors for improved grasping control in prostheses.

Current tactile sensors harness the increased pressure sensitivity and high-fidelity signal resolution to allow for the classification and discrimination of surface textures. This is done through an interdisciplinary application of digital signal and waveform processing as well as statistical and machine learning techniques. This texture information is still not recognizable directly by the nervous system. It is therefore of high interest to further realize neuromorphic encoding to properly package material surface characteristics into a language that the peripheral nervous system can perceive and central nervous system can comprehend.<sup>44</sup>

To reiterate, after a given sensor detects its respective percept, the generated signals will be processed and relayed to the user. Implanted electrodes can interface directly with intact afferent neurons, mimicking stimuli that would be perceived as sensory stimulations from the lost limb, creating phantom limb stimulation, or that can otherwise be used to relearn percepts in order to evoke sensory replacement. Non-invasive extra-dermal systems have also been developed to provide sensory replacement.<sup>23</sup> In addition, surface electrode systems have been used to stimulate the phantom hand rather than just replacing lost sensations with new ones imparted on the residual limb.<sup>3</sup>

This article aims to provide a comprehensive review of current technologies and new developments of smart prostheses focused on the last 5 years. We intend to confer a broad overview of essential concepts in tactile sensation, texture recognition, and sensory feedback strategies that have been either used in smart prostheses or have significant potential for translational applications through their intended design.

## MATERIALS AND METHODS

The PubMed and Engineering Village databases were used to search for studies involving the development and testing of novel prosthetic sensors, signal processing techniques for texture recognition, and sensory stimulation techniques for neural prostheses. Included in the primary research papers were 13 studies regarding to prosthetic sensors, 14 on texture recognition signal processing in prostheses, and 27 on sensory stimulation techniques. An emphasis on studies from the last 5 years was made, with earlier studies included to show foundational aspects of current designs and concepts. The literature searches and data collection were completed by a group of seven independent reviewers. First readings were divided topically for individuals and screened for use in the review, which were then cross-referenced by the remaining reviewers.

## PROSTHETIC SENSORS

Prosthetic sensors are used to detect external stimuli such as force and pressure at the fingertips of prostheses. Common electronic components that detect force and transduce the information directly to electrical signals are the most apparent and available solutions. These synthetic sensors are often adapted and modified to allow for more specificity and sensitivity at the range that would be common for human interaction. Custom sensors that are designed based on biological components of the hand are referred to as biomimetic sensors.

### *Synthetic Sensors*

Synthetic sensors detect contact forces by measuring internal changes in resistance, capacitance, or inductance due to an externally applied force. The sensitivity and working range of these sensors can depend on which method of measuring the applied force is used. However, the working range can be improved by modifying the contact surface with more compressive materials such as synthetic polymers. While synthetic sensors aim to replace lost sensory information, the design strategy is not inspired by the lost biological skin or afferent fibers. Instead, this group of sensors leverages the availability and functionality of common electrical components that are manufactured on an industrial scale.

Resistive sensors measure internal changes in resistance due to an externally applied force, typically resulting in the temporary physical deformation of the sensor before returning to its passive state when no loading force is applied. Resistive sensors have been used to detect the normal force, shear force, lateral strain, and bending strain through the conversion of such mechanical changes into an electrical resistance.<sup>8,12,31,38,39,48,55,63,65,69,73,76,81</sup> Resistance changes can be measured through Micro-Electro-Mechanical Systems (MEMS), strain gauges, or fluid-based designs that incorporate piezoresistive elements. Certainly, sensors that are more useful for prostheses are those which are more sensitive to a range of low-impact forces that would typically be experienced at one's fingertips. Therefore, custom sensors have been developed. One highly sensitive sensor design comprised of three different elastomers: (1) 30  $\mu\text{m}$  strain gauge made from carbon-black-doped Polydimethylsiloxane (PDMS), (2) interconnect using carbon-nanotube-doped PDMS, and (3) insulating PDMS matrix substrate that resulted in a sensor with a Young's modulus of 244 kPa, which is a similar stiffness to skin.<sup>38</sup> The use of a Wheatstone bridge circuit to measure the resistance changes as well as the serpentine

implementation (Fig. 1a) of the elastomer components helped create a more sensitive sensor. Another synthetic resistive sensor used two interlocking arrays of polyurethane-based nanofibers coated with platinum to measure nanoscale deformations (Fig. 1b).<sup>38,48</sup> Mechanical loads such as pressure, shear, and torsion forces were extrapolated and able to be distinguished due to the two interlocked layers of the nano-hair structure. Highly-oriented carbon nanotube (CNT) fibers have been used to create strain gauge sensors to detect uniformly distributed stress.<sup>55</sup> The CNT sensors provided high sensitivity, fast response times, and were durable for use in motion detection systems.

Conductive fluids have also been used on other custom-built resistive sensors where mechanical load causes changes in resistance through fluid displacement. A rigid core with outward-facing electrodes can be surrounded by a compressive sheath with conductive particles, creating a sensor that responds to applied forces by measuring impedance changes imposed by the altered fluid path. A solution of aqueous NaCl at  $0.75 \text{ g L}^{-1}$  is poorly conductive, but allows for a useful detection of forces from 0.01 to 40 N by creating an impedance range of 5–1000 k $\Omega$  when implemented along with a linearly grooved external surface.<sup>69</sup>

Another sensor measures pressure and shear forces independently using an elastomer with a central chamber filled with eGalin, a liquid-metal alloy. A central chamber is linked to two reservoirs through microchannels. Deformation of the elastomer through mechanical load created fluid movement, which could be measured by using changes in impedance. Depending on the direction of fluid movement, direct pressure (force) vs. sliding contact (shear force) could reliably be distinguished.<sup>73</sup>

Capacitive sensors that measure changes in capacitive coupling across materials have been used in designs that allow for pressure detection, shear force sensing, and texture recognition.<sup>43,44</sup> Polymers such as PDMS have been used in mesa micro-structures to achieve flexible and sensitive sensors.<sup>27,39,81</sup> To increase capacitance sensitivity, the PDMS dielectric layer can incorporate different micro-structures such as pyramids and v-shaped grooves (Fig. 1c). One sensor used two conductive plates composed of flexible polyethylene terephthalate (PET) substrate embedded with copper electrodes.<sup>27</sup> For texture recognition, a capacitive sensor was designed using a linear array of MEMS sensors in two-layers. The sensor array consisted of an upper diaphragm with highly doped single crystal silicon, placed above a lower highly doped sil-

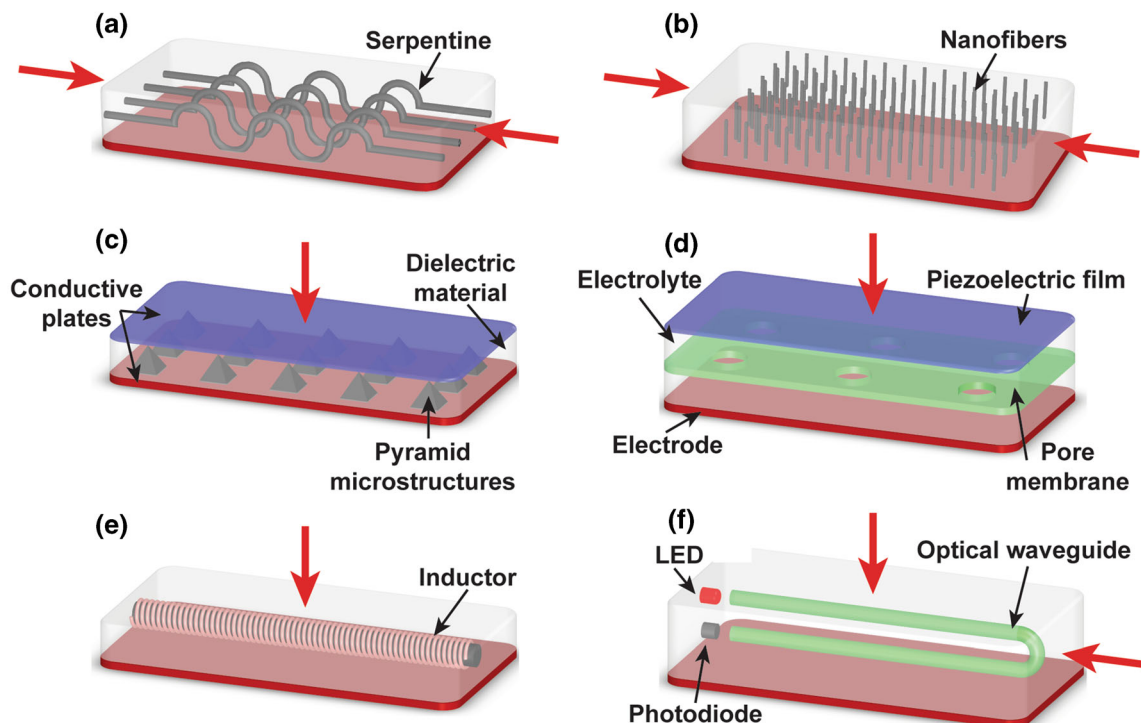


**FIGURE 1.** Representations of the different synthetic sensors: (a) serpentine and (b) nanofiber elements of strain gauges in resistive sensors,<sup>38</sup> (c) pyramid microstructures in the PDMS layer to create a more sensitive capacitive sensor,<sup>27</sup> (d) pore membrane in a piezoelectric sensor to create artificial ion channels,<sup>74</sup> (e) inductor in an inductive sensor to create digital-frequency signals,<sup>70</sup> (f) optical waveguides in optical sensors that can be embedded in prosthesis.<sup>78</sup> Red arrows indicate the directions of deformation that the sensors detect.

icon electrode, separated by an air cavity.<sup>43,44</sup> In response to an applied force, the deformation of the diaphragm causes the capacitance to change.

Piezoelectric materials that naturally transfer mechanical stress into an electrical potential are another common sensing element. Piezoelectric materials such as polyvinylidene fluoride (PVDF) have fast and accurate responses to high-frequency vibrations (Fig. 1d). One simple piezoelectric sensor embedded a PVDF film bonded with electrodes in an elastomer for advanced prosthetic limbs. The bio-inspired tactile sensor converts the sensor response into spike trains using a spiking neuron model in order to simulate mechanoreceptors in the skin.<sup>74</sup>

Another more complex sensor combines a piezoelectric film with an artificial ion channel composed of a double-layered polyaniline (PANI) solution split by a porous PCTE membrane and by a gold-coated PVDF film on top of an AL/C electrode.<sup>16</sup> When pressure is applied to the PVDF, a voltage is generated. Within the PANI, this voltage induces a charge density and electrical potential. The voltage change in the PVDF film is large and quick, whereas the voltage at the PANI interface is smaller and sustained for the duration of contact with a surface. These voltages were converted to frequency signals *via* a voltage-controlled oscillator.

Field-effect transistors detect mechanical deformation through its effect on the electric field within the device, which changes the flow of charge in the semiconductor channel.<sup>32,76</sup> Organic field-effect transistors (OFETs) in tactile sensors use organic semiconductor channels such as carbon nanotubes, conductive polymers, graphene, and metallic nanowires.<sup>70</sup> One such sensor was developed by integrating micro-structured PDMS films into OFETs as the dielectric layer.<sup>41</sup> Micro-structured PDMS films yielded higher sensitivity to pressure and faster response times to pressure release when compared to unstructured film. These PDMS films enable more direct measure of pressure and allow for greater sensitivity that also reliably mimics the level needed for prostheses. By modifying the shape of the PDMS structures, such as pyramidal-like structures, a higher sensitivity and pressure range can also be achieved.

Inductive sensors detect the applied load as a modulation of the mutual inductance of a magnetic field between two coils. These sensors tend to be large and complex, resulting in lower reliability.<sup>39,65</sup> A tactile sensor was developed by embedding a polymer membrane containing magnetic particles above an inductive magnetic sensor (Fig. 1e).<sup>70</sup> The sensor was constructed of a Cu coil wrapped around a Co-based amorphous wire, which is a type of giant magneto-impedance material chosen for its sensitivity. To allow

for easy deformation of the membrane due to pressure, the polymer membrane was placed in an air gap, which helps the magnetic sensor detect changes in the magnetic field. The inductive magnetic sensor formed part of an LC circuit, so the changes in magnetic field were directly transduced into digital signals, manifesting as changes in oscillation frequency.

Optical sensors have been used for tactile signal transduction, measuring optical variations across semi-transparent media due to physical deformation upon contact and pressure.<sup>20,39,65,76,81</sup> Optical sensors have a large form factor, yet maintain high sensitivity and resolution, while being immune to electromagnetic interference from nearby sources.<sup>20,65,81</sup> A prosthetic finger was developed using a sensor with a looped optical waveguide, which is the combination of an optically-focused light-emitting diode (LED) on one end and a sensing photodiode to sense light intensity on the other end (Fig. 1f).<sup>78</sup> The changes in light intensity were proportional to the elongation of the finger. These sensors are subject to less hysteresis and time response than other types of devices due to the immediate response of light intensity to strain in the device.

Sensors that utilize the triboelectric effect, which is the induction of electrical potential through moving specific materials across one another or through separation, present the advantage of not requiring an external power source. One example of the triboelectric effect is static electricity. Using this triboelectric principle, a self-powered, flexible tactile sensor was developed that generates a voltage response from physical contact.<sup>79</sup> Contact electrification is provided by a nano-wire layer of fluorinated ethylene propylene (FEP), which generates the electrical charges, thus determining the sensitivity of the device. Upon contact with an object, the electrode becomes negatively charged. After separation, the FEP remains charged for an extended period and generates a net electrical potential, which can be measured as a voltage across the electrode. When Fluorine contacts many materials, it gains a negative charge. This causes FEP to have very strong triboelectric properties.

### *Biomimetic*

The design of prosthetic sensors has also been directly inspired by the biological components that are aimed to be replaced. Prosthetic sensors should also mimic the biological characteristics of the skin, including signaling mechanisms,<sup>16,63,73,74</sup> structure,<sup>8</sup> and mechanical properties.<sup>31,73,82</sup> The human glabrous dermis layer contains four types of low threshold mechanoreceptors (LTMRs), categorized into slow-adapting (SA) and fast-adapting (FA), that measure



mechanical stimuli (Fig. 2). Among the four LTMRs, Merkel cells (SA1) and Ruffini endings (SA2) produce sustained signals throughout mechanical stimulation. This allows these receptors to measure static force and strain from prolonged contact. Meissner corpuscles (FA1) and Pacinian's corpuscles (FA2) produce dynamic signals and are more involved in detection of features of an object and vibration.<sup>1</sup>

Piezoresistive sensors have been used in the design of organic prosthetic sensors that mimic the biological signaling activity of SA and or FA mechanoreceptors, forming a digital mechanoreceptor. The transduction from analog sensor reading to spiking signals was achieved either through an electronic circuit or a software model (Fig. 3). An oscillating circuit that produced a periodic square wave was used to encode physical force stimuli into digital signals.<sup>63</sup> Pyramidal micro-structures were constructed from polyurethane elastomers with embedded carbon nano-tubules. This combination of piezoresistive sensors and organic oscillators enabled varying sensor output frequencies, which mimicked SA mechanoreceptors. Increased sensitivity and working range of the sensor was achieved by reducing the effective Young's modulus and concentrating the electric field.

Another sensor that was designed to mimicked the SA signaling mechanism uses conductive microfluids encapsulated in polymer film to form a hemisphere.<sup>73</sup> The volume of fluid and diameter of the hemisphere could be adjusted to control the sensitivity of this fluid-based resistive sensor. Normal forces and shear forces were detected by measuring the concurrent resistance changes, which showed a similar profile to SA skin

receptors. The activity of FA receptors has been reproduced by a sensor design that used PVDF as the conductive piezoelectric material and PDMS as the coating.<sup>74</sup> Continuous electrical signals were converted into spike trains with variable frequency, based on a neuron model that describes the current change across FA mechanoreceptors. This conversion from voltage output of the sensor to a spike train mimicked FA receptor response (Figs. 3d and 3f).

More recently in 2018, a self-powered piezoelectric sensor achieved properties of both SA and FA mechanoreceptors. To realize both SA and FA responses, this sensor needs to generate two types of voltage outputs, one corresponding to SA and the other FA, in response to pressure.<sup>16</sup> The sensor consists of a piezoelectric film made with gold and PVDF as well as an artificial ion channel made with an electrolyte (PANI solution) and a pore membrane. Applied pressure to the sensor deforms the piezoelectric film, allowing for the encoding of an FA response. As contact is maintained, ion movement through the electrolyte in the membrane occurs, creating a sustained SA response. The sensor was demonstrated to identify mechanical stress and detect grasping events such as slipping objects.

Prosthetic sensors have also been designed based on the surface structure of fingerprints. A flexible tactile sensor has been developed with microscale pyramids on both the outer layer in contact with the object surface and between the inner layers of the sensing element (Fig. 4).<sup>8</sup> This sensor, with the outer pyramid layer inspired by shaped grooves of fingerprints, was made of single-walled carbon nanotubes (SWNTs),

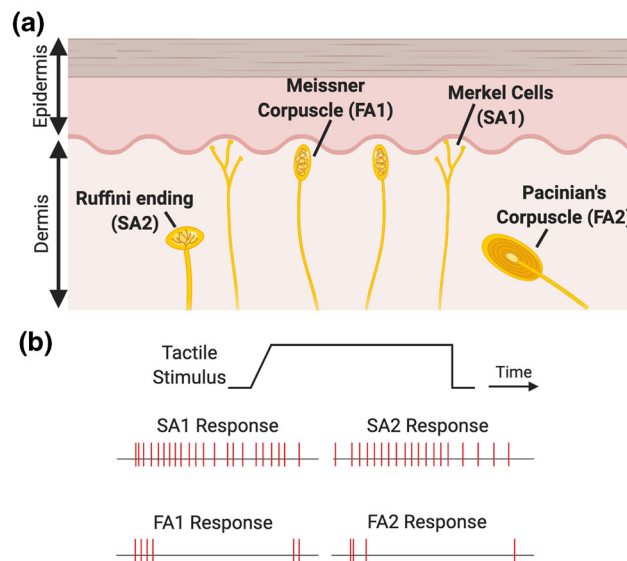


**FIGURE 2.** Schematics of human glabrous skin mechanoreceptors and firing patterns. (a) Glabrous skin contains four types of LTMRs: FA1, FA2, SA1, and SA2. (b) In response to a tactile stimulus, the four LTMRs show different firing patterns.

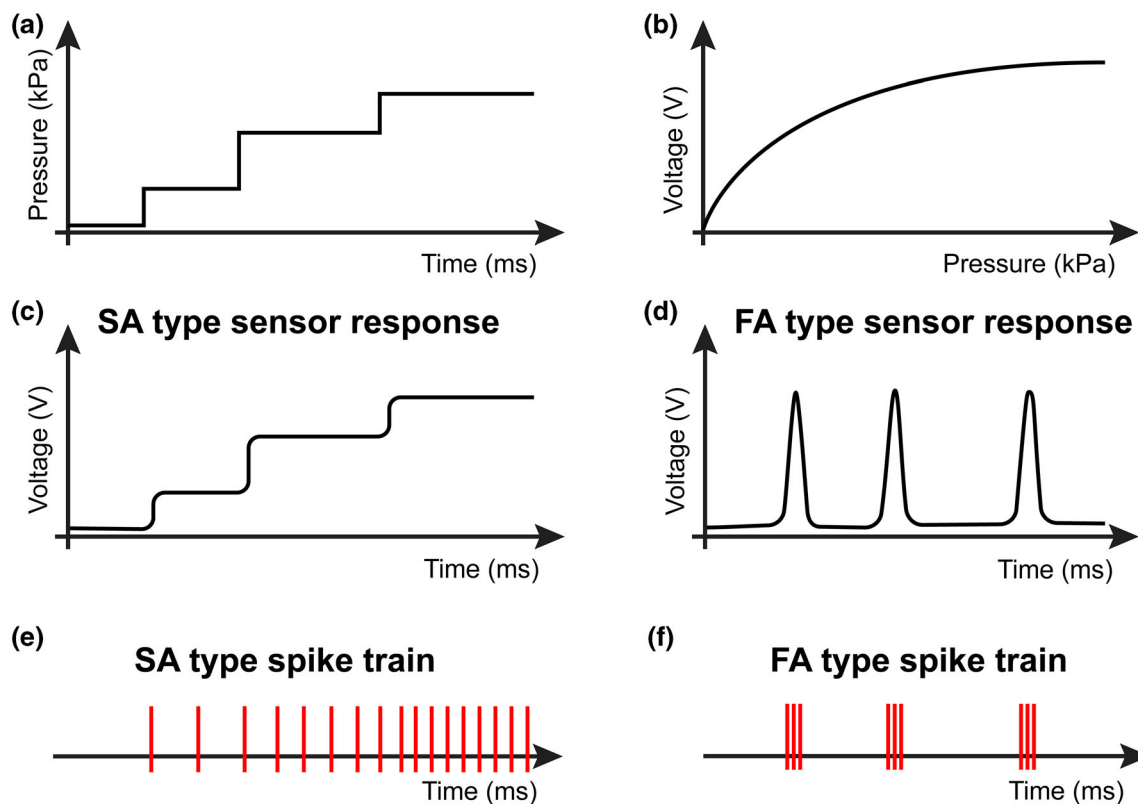


**FIGURE 3.** Schematic of sensor responses that mimic mechanoreceptor signaling mechanisms. Given an example of (a) applied pressure change with time and (b) the corresponding sensor voltage response with pressure, (c) a sensor that mimics the SA signaling mechanism shows a profile that gradually changes with applied pressure. (d) A sensor that mimics the FA signaling mechanism shows voltage changes only when pressure changes. (e, f) Converted to spike trains, the SA type sensor shows firing pattern similar to SA mechanoreceptors and the FA type sensor shows firing pattern similar to FA mechanoreceptors.

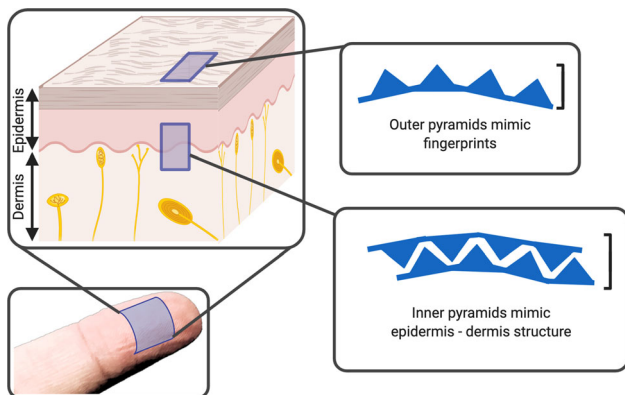


**FIGURE 4.** Structural layout of sensors (right) that mimic different parts of the skin. Outer pyramids mimic grooves on the skin surface and interlocking pyramids mimic the connection between epidermis and dermis.

polyethylene, and PDMS. Two inner layers of SWNT formed pyramids that were organized into an interlocked layout, allowing for the sensor to detect changes in both normal and shear forces. The use of pyramidal structures allowed for high sensitivity, as the tip of the

pyramid deforms more easily upon applied force than a smooth surface with more direct contact and rigidity.

Biomimetic sensors have also sought to copy the compressive nature of skin along with its ability to stretch. Most tactile sensors described so far have used stretchable materials such as elastomers to mimic basic viscoelastic properties of the skin surface. However, the sensing elements themselves were underneath this skin layer. Flexible sensors can be manufactured to accommodate skin-like mechanical properties across the sensor itself. Silicon-based circuits can be prestrained to provide sustained force detection in thin, deformable layers while under strain due to applied forces.<sup>29</sup> The same pre-straining strategy was applied to develop a skin-mimicking, stretchable sensor using silicon nano-ribbons covering an entire artificial hand. Local curvature of the ribbon is site-specific and can be calibrated to conform with the curvatures of the prosthetic hand, thus corresponding to the natural elasticity of the hand region. A greater curvature corresponds to heightened elasticity and lowers piezoresistive sensitivity.<sup>31</sup>

The extent of biomimicry in prosthetics is not limited to mechanical properties and sensory end organs. The premise of wound healing has also been explored in terms of prosthesis healing. Made of a dynamic, covalent thermoset doped with silver nanoparticles, a re-healable sensor was able to reform its original structure after external damage due to an abrasive cut. Application of a polymerization compound solution and heat allowed for covalent bond exchange reactions at the wound site, enabling the healing of the sensor surface.<sup>82</sup> Although the capacitance profile of the original, undamaged sensor was not completely retained after the healing process, it did allow for similar object detection.

## TEXTURE RECOGNITION

One of the major decoding goals of raw prosthetic sensor output is for the texture of objects to be accurately identified. The identification of physical properties of objects improves grasping tasks by moving from an all or nothing grasping approach with full power, to a smoother and more continuous control of grasping forces based on the given system feedback. Object stiffness and texture can be used to improve the breadth of sensations replaced for amputees while improving grasping tasks.

Many of the currently available texture sensing technologies and their performances at detecting a variety of surfaces are discussed below. Additionally, the use of classification algorithms to connect the signals to actual surfaces will briefly be discussed, as it serves as the final performance metric to understand the effective sensitivity of a tactile sensor. The sensor technology described above has been focused on increasing signal sensitivity for accurate detection of texture information. Texture detection studies use different types of tactile sensors to (a) scan surfaces in the temporal domain, (b) process temporal signals to determine characteristic patterns of surfaces, and (c) utilize classification algorithms to correctly identify and categorize textures. A comparison of recent studies in texture sensor and recognition is reported in Table 1.

### *Tactile Texture Sensing*

Piezoresistive (PR) sensors are commonly used in tactile sensors for texture detection.<sup>8,14,15,30,35</sup> MEMS have wide applications for creating highly sensitive tactile sensors that convert mechanical deformations into electrical resistance through multi-axial piezoresistive sensors. Deflection of these resistors, when scanning over surfaces, can define micro-structural

differences as the sensor moves across the surface that are indicative of specific texture features. This method can detect pressure changes of fine weave patterns of paper textures.<sup>30,35</sup> Other MEMS-based capacitance sensors with a linear array of four tactile sensors were able to detect surface patterns as small as 200  $\mu\text{m}$  and were capable of obtaining characteristic frequencies that encode texture differences between smooth PDMS surfaces and nylon. Distinct characteristic signals could be detected for each texture after the multi-array sensor signals were fast Fourier transformed, exhibiting the capability of multi-array sensor configuration to capture both temporal and spatial information. This would enhance the potential for texture pattern detection significantly.<sup>44</sup>

Novel fingerprint-inspired SWNTs/PDMS composite piezoresistive sensors are flexible, able to discern a useful range of pressures during scanning movements (45–550 Pa), and can detect changes in resistance from 0 to 2500 Pa. A double-sided, double-layered, interlocked pyramidal SWNT micro-structures can detect even minute changes in shear force. Even fine periodic texture patterns with 15  $\mu\text{m}$  interval spacings were detected with discernable output signal changes. This feat highlights the SWNT's high recovery rate after shear force, attributed to the pyramidal microstructure design. Minute differences in various fabric textures could easily be identified based on their output signals.<sup>8</sup>

A composite of graphene flakes and polyurethane sponges have been integrated for use as an improved conductive graphene piezoresistive sensor.<sup>15</sup> The sponge material is slow to return to its original shape after deformation. Despite this extended time dependency, the signal acquisition still maintained low enough noise artifacts vs. the actual signal to distinguish characteristic FFT peaks. The graphene composite allowed for distinguishable FFT characteristic signals for ridge (grooved surface structures) detection with a minimum of 200  $\mu\text{m}$  separation on fabricated PET material.<sup>14</sup>

Piezoelectric (PE) sensors using PVDF have exhibited sensitivity to external input that results in distinguishable voltage signals. One of the main characteristics of PVDF is the ability to mix other chemical compounds into the structure of PVDF. The introduction of impurities dictates the “roughness” of the PVDF film and determines the piezoelectric sensitivity to external surfaces. A PVDF film was used to determine the differences in different weave fabrics. Detection and classification of different surface types were done by extracting features from the output frequency and classified through an unsupervised k-means clustering algorithm.<sup>59</sup>

TABLE 1. Comparison of texture recognition techniques in recent works.

Ref.	Sensors	Materials	Textures detected	Algorithms/protocols	Accuracy	Res.
30,35	PR	NiCr, Silicon MEMS, Strain Gauge	10 different papers with varying textures patterns, 5 Texture Patterns	Multilayer perceptron, maximum likelihood	53–80%	830 $\mu\text{m}$
A combination of MEMS and strain gauges were used to make sensors that can detect roughness events from various types of paper textures with a minimum periodic weave pattern of 830 $\mu\text{m}$ at a scanning velocity of 7.6 and 3.8 $\text{cm s}^{-1}$ . For the task of classifying 10 differently textured patterns, the accuracy from capacitance signal derived texture features were between 53 and 67%. For the detection of 5 texture patterns, the accuracy greatly improved to 60–80%						
8	PR	SWNTs/ PDMS	Silk fabrics, braille	FFT		15 $\mu\text{m}$
The single-walled carbon nanotube with cross-linked micro pyramidal flexible sensor array exhibits extreme sensitivity to pressure and can detect texture surfaces by detecting the shear force changes through surface interactions. Output signals were Fast Fourier transformed and have exhibited significant signal structural differences even in silk fabric and braille textures as small as 15 $\mu\text{m} \times 15 \mu\text{m}$						
14,15	PR	Graphene Sponge	PET flexible ridges	FFT		200 $\mu\text{m}$
Two single-layered graphene sheets are placed parallel to each other on either side a polyurethane sponge with high sensitivity pressures detectability ( $-0.24$ – $0.039 \text{ kPa}^{-1}$ ) can detect shear force changes between the two graphene layers in conjunction with the properties of graphene itself. This application of PR can detect ridge spacing on PET as close as 200 $\mu\text{m}$ . Although the FFT signals are noisy due to the slow recovery time of a sponge material, characteristic peaks can still be detected that align with each corresponding material gap width						
59	PE	PVDF	5 types of fabrics including silk, cotton, and wool	RBF, k-means clustering	96–100%	60 $\mu\text{m}$
A single layer of PVDF with roughness $< 15 \mu\text{m}$ was used to quantify textures of different types of fabrics with periodically patterned weaves as small as 60 $\mu\text{m}$ . The frequency output from the PVDF sensor from each of the different fabric was used to classify the frequency extracted features from each of the 5 fabrics by using a neural network implementation of K-means clustering algorithm (RBF). The high accuracy signifies that the signals that the features were derived from were sufficiently different for each fabric but may mean that since the fabrics were significantly different, the classification task itself was too simple.						
52	PE	2-layer PVDF	15 graded polished metals	KNN, SVM, ELM	57–73%	0.44 $\mu\text{m}$
51	PE	2-layer PVDF	8 graded ridged textures	DWT, KNN, SVM, ELM	80–97%	0.04 $\mu\text{m}$
Two PVDF films were placed in a perpendicular arrangement to allow for increased signal acquisition (in two axes) and to more adequately detect vibrational differences during the scanning task over surfaces of metals polished with different sandpaper gratings. Similar to <sup>58</sup> signal pre-processing and statistical feature extraction was performed but due to the much more difficult task of determining the degree of polish of metals, the accuracy of the classification tasks using KNN, SVM, and ELM were much lower than classifying fabrics						
26	PE	Multi-strain gauge, PVDFS	8 surfaces: carpets (2), sponge, tiles (2), vinyl, wood, fabric	Decision Trees (Naïve Bayes, boosted tree)	80–100%	
Multi-strain gauges and PVDFs were laid between two silicon layers. The strain gauges serve as slow-adapting mechanoreceptors that provide resistance change signals when under strain. PVDFs act as fast-adapting mechanoreceptors that provide electric charge response to pressure. The number of PVDF and strain gauges ranged from 2 to 8 and were randomly placed between iterations. Through the inclusion of a majority voting algorithm, classification accuracies were improved when applied to the decision tree algorithms						
44	C	Silicon MEMS	Smooth PDMS surface, polycotton, nylon	FFT		200 $\mu\text{m}$
Signals from a linear array of 4 MEMS capacitance sensors were used to discern the course to fine texture differences of periodic gratings in PDMS surfaces and fabrics down to 200 $\mu\text{m}$ . The use of a multiarray of sensors allowed for both the capture of temporal and spatial information shown through the ability to capture differences in the fast Fourier transformed signal peak characteristics						

Ref. References, Res. Resolution, PR piezoresistive, PE piezoelectric, C capacitive, RBF radial basis function networks.

Flexible two-layered PVDF sensors showed enhanced sensitivity and higher resolution (0.43  $\mu\text{m}$ ), with capabilities to differentiate between texture signals of polished metal surfaces. The perpendicular orientation of the two PVDF films allowed for increased signal acquisition and the ability to sense vibrational differences between the two sensors during scanning. Despite the higher sensitivity PVDF sensor arrangement and the use of various machine learning algorithms, the accuracy of classifying polished metal surfaces was much lower than that of fabric detection.<sup>59</sup> This could be attributed to the increased innate difficulty of sensing the minute sandpaper gratings

between polished metals, which would even prove to be challenging for a human finger tip.<sup>51,52</sup>

Additionally, a multi-modal sensor array of multiple gauge sensors and PVDFs was able to identify the differences between various materials such as carpet, tile, wood, vinyl surfaces, and fabrics based on extracted features from texture information. Resistance changes were captured by strain gauges and electric potential changes were captured by PVDFs in response to strain and pressure inputs. Although this classification task was simpler, the output signals were pre-processed and applied to more sophisticated learning algorithms (Decision trees, Naïve Bayes, boosted tree).



When combined with their voting algorithm, the classification scheme accuracy reached 80–100%.<sup>26</sup>

### *Signal Processing and Classification*

Signal processing and feature extraction algorithms are crucial to properly decomposing and translating tactile sensor signals into useable texture features. General statistical algorithms and machine learning techniques have been applied to the problem of classifying textures and surfaces. The Fast Fourier Transform (FFT) and Discrete Wavelet Transform (DWT) are leading techniques for preprocessing and simplifying signal output from sensors. Statistical and learning algorithms including decision trees (DT), support vector machines (SVM), extreme learning machines (ELM), gradient boosting machines (GBM), maximum likelihood estimations (MLE), k-means clustering (KM), and k nearest neighbors (KNN) are used to categorize and identify textures.

The FFT is most commonly used for temporal signals from sensors. The FFT identifies characteristic surface features, including ridges and depressions, by correlating the frequency of pressure changes across a tactile sensor as it is scanned across an uneven surface.<sup>8,14,15,26,44,52,59,75</sup> The FFT captures the prominence of different frequencies of pressure changes, which can be directly used for surface classification or as a subset of features in machine learning strategies.<sup>8,14,15,51</sup>

Wavelet filters can also be applied in signal processing of raw signals, referred to as discrete wavelet transforms (DWT), creating high-pass and low-pass filters which can retain the original frequency and temporal information. DWT results can then be used for feature extraction for machine learning strategies, similarly to FFT. In practice, DWT is often only used when FFT results fail to produce satisfactory discrimination of surfaces.<sup>28</sup>

Classical statistical features of the raw signal have also been used to characterize surfaces and provide engineered features for texture recognition machine learning algorithms. Useful statistical features include variance, standard deviation, power, kurtosis, mean, median, max, mode, and range.<sup>22,30</sup> A combination of features from FFT, DWT, statistical measures, and raw temporal signals provide a more comprehensive description of surfaces. Providing a greater quantity of descriptive data often improves the accuracy of machine learning strategies. Signal data can also be separated based on temporal and frequency measures in an attempt to retain features for each domain space.<sup>51</sup>

Various feature extraction techniques and machine learning algorithms have been used in attempts to reliably identify textures (Table 1). Supervised ma-

chine learning algorithms with labelled training data (DT, SVM, ELM, GBM) have dominated the literature (Table 1). Even those that would typically be unsupervised methods (KM, KNN, MLE) are applied with integrated label information to perform a supervised classification task (Table 1).

The performance of each of these algorithms mentioned in the literature includes area under the curve of the receiver operating curve (AUROC), sensitivity, specificity, and accuracy. Accuracy is often used as the measure of success for a machine learning application, but it does not incorporate the possibility of overfitting to the data or whether the model has used the expected features. Low accuracies can also be indicative of particularly difficult classification tasks. Identifying the difference between metals polished with different sandpaper grits is more difficult than identifying wool vs. metal or wood.<sup>30,75</sup>

Recent literature highlights the successful ability of tactile texture sensors capable of detecting microstructures ( $> 0.4 \mu\text{m}$ ) and displaying extreme sensitivity to imperceptible pressure changes during scanning<sup>51</sup> (Table 1). The raw electrical signals have been shown to be characteristic of specific texture surfaces with preliminary classification tasks showing acceptable discrimination among tested materials (53–100%) (Table 1). While being able to differentiate microstructures may not be necessary for prostheses, these studies show the ability of well-designed machine learning strategies to directly use raw signal data rather than engineered features.

Advances in computational resources and applied algorithms have allowed for the high sampling rates and real-time processing needed for responsive, closed-loop feedback in experimental prostheses. Processing sensor signals during object grasping tasks and encoding for slip detection has been used to provide stimulation feedback *via* cuff and intraneural electrodes. The stimulation feedback enhances efficacy of grasping and object manipulation tasks while using a myoelectric prosthesis, controlled by muscular flexion in the residual limb.<sup>80</sup> Enhancing closed-loop control of prostheses, from stimulation to myoelectric control and then adjusting the stimulation with processed sensor signals, has been an active goal in experimental prosthesis research.

Closed-loop prosthesis control may be further enhanced with automatic grasping force and grip type modulation by the prosthesis itself. Past prostheses have used automatic full-force grasping without sensor feedback, making it difficult to grasp and manipulate a more complete variety of objects. Using processed signals from prostheses allows for a secondary closed-loop system within the prosthesis itself to modulate hand positions and grasping forces.<sup>77</sup> Assistive, semi-

autonomous prosthesis control can also aid in bimanual object manipulation for patients with an intact arm. Detection of bimanual tasks requires wearable sensors on the healthy arm, but allows for bimanual task to be completed more quickly and with less cognitive demand.<sup>68</sup>

### *Other Applications of Texture Recognition Technologies*

Active progress in virtual reality and human-computer interface, with respect to texture recognition, has included the use of texture databases, object shape and surface recognition, and haptics to enhance the user's perception of the virtual space. These advances could be directly applied for the benefit of prostheses users in order to reestablish a sense of touch while interacting and perceiving their environment.

In order to convey the similarity and differences of textures, multidimensional scaling (MDS) is used to characterize textures on the axes such as patterns, level, and dynamic friction.<sup>45</sup> This allows for the creation of well-differentiated textures to visualize and interact with in the virtual space. To render parameters for texture perception, an open-source framework, Chai3D, is used for computer haptics, active visualization, and interactive real-time simulation ([www.chai3d.org](http://www.chai3d.org)).<sup>45</sup>

Model-based texture recognition systems use an image of an object to classify the surface texture.<sup>37</sup> The Columbia-Utrecht (CURET) database contains 61 real-world 3D texture surfaces that has been used to test the ability of algorithms and texture perception methods (<http://www.cs.columbia.edu/CAVE/software/curet/>).<sup>19</sup> High recognition rates of CURET's surface textures is possible by combining feature grouping and dimensionality reduction of the object's image.<sup>19</sup> Another study compared direct image feature prediction and image prediction *via* surface feature prediction by testing them over 35 surface textures.<sup>37</sup> Image prediction *via* surface feature prediction infers the surface shape of a virtual object followed by the intensities of the features on that surface. This method produced a larger error in recognizing surface textures but was better at predicting the shape. These texture prediction algorithms can be adapted for use in prosthesis texture recognition.

## SENSORY STIMULATION

The information gathered from prosthetic sensors is encoded and used to stimulate afferent nerve fibers directly through implanted subdermal electrodes or through less invasive measures using extra-dermal stimulation approaches. Major developments in skin-

surface sensory substitution techniques and implanted nerve electrode designs have been made in the past 5 years. As such, we focus on them in the report here.

### *Extra-dermal Stimulation*

Activation of the sensory system can be achieved through non-invasive techniques that stimulate the skin surface or even directly stimulate the underlying afferent nerves. The end-results are unique in the evoked perception. While skin surface stimulation will be felt locally, targeting the underlying afferent neurons that once innervated with the lost hand or finger can produce sensations of the phantom limb being directly stimulated. When non-invasively stimulating the skin, percepts could be learned and correlated to different environmental cues, such as vibration on the upper arm upon contact of the prosthetic fingers with an object, through the process of sensory substitution. Alternatively, extra-dermal stimulators can be used to non-invasively target the underlying afferent fibers below the skin, providing sensation to afferent fibers that were once connected to the lost limb. When these nerve fibers are stimulated in this manner, sensations are perceived to originate from the hand or lost limb, even though the electrodes are placed elsewhere (Fig. 5).<sup>23</sup> The activation of these afferent fibers is referred to as phantom limb stimulation and is often used to highlight this difference in neuronal targeting. These two strategies can be classified as extra-dermal since the stimulators are located on the surface of the skin rather than being surgically implanted along peripheral axons, which is characterized as subdermal stimulation.

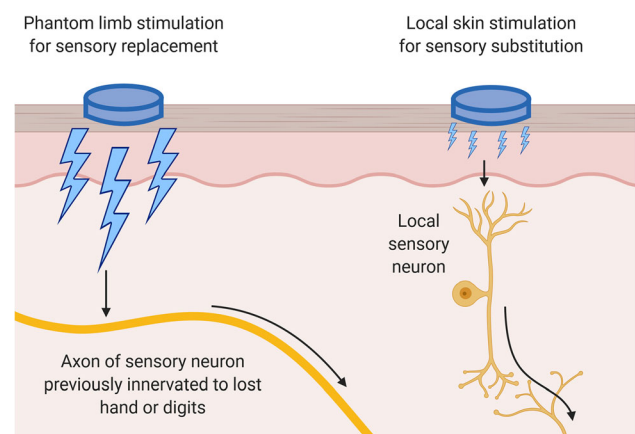


**FIGURE 5.** Recruitment of sensory neurons from the lost limb can result in phantom limb stimulation for more natural sensory replacement. Localized stimulation recruits local sensory neurons, resulting in sensory substitution, which can be used to relearn sensory associations.

Electro-tactile feedback techniques use surface electrodes to indirectly stimulate the afferent sensory nerves under the skin. The electrical signal is introduced at the skin surface which can be directly sensed on the skin for sensory replacement or can alternatively be used to target the underlying axons that represent the phantom limb. Extra-dermal electro-tactile stimulation is often referred to as transcutaneous electrical nerve stimulation (TENS). Sensory substitution has been achieved with an electrode array consisting of four channels that are placed along the medial center of the upper arm. The electrodes can deliver both pressure and slip feedback to the subject by changing the frequency and amplitude of the current and through cyclic activation patterns. When testing the efficacy of using slip, pressure, and visual feedback, it was found that slip feedback was the most useful for maintaining a grasping force while a combination of slip and pressure feedback allowed for the most rapid transition from rest to grasping at the necessary force.<sup>71</sup>

Sensory substitution can also be used for more severe injuries where sensory perception along the entire arm is completely lost. Electrical transcutaneous stimulation along the back of the neck could particularly benefit patients with certain spinal cord injuries. The encoding of tactile grip force and hand aperture through electrical stimulation along the neck with four discrete contact sites have been used to provide force and proprioceptive information.<sup>3</sup> The ability to accurately determine the weight and size of an object increased with training over 5 days, but on average, objects were properly identified only 49% of the time. It is expected that further training would improve object discrimination, as a machine learning model was able to classify the objects with 100% accuracy when using the stimulation parameters as training features.<sup>3</sup>

Still, more extensive surface electrode patterns have been designed, including a 16-point contact system that wraps around the residual limb circumferentially.<sup>66</sup> The increased number of electrodes allows for more stimulation contacts and a greater number of associated percepts. However, there is a limit to the useful density of electrodes for sensory replacement or phantom limb stimulation. If two neighboring electrodes are too close to be differentiated, then they won't be useful as separate stimulators. By using circumferentially placed electrodes, the spacing of electrodes is more distinguishable by users than denser grid patterns.<sup>66</sup>

External transcutaneous stimulators can be used to target the median and ulnar nerves. Rather than being perceived as local electrical stimulation at the electrode sites, subjects feel the sensation along their hand with finger-level discrimination. The phantom hand is a concept used to describe the ability of an amputee to

perceive sensations as originating from the lost hand. A  $2 \times 8$  electrode grid placed below the bicep, along the medial side of the upper arm, has been used to stimulate these afferent nerve fibers, providing perceived sensations on individual fingers by altering the active electrode pairs on the upper arm.<sup>58</sup>

Artificial activation of the phantom hand through transcutaneous electrical nerve stimulation can also be used to reinstate other percepts beyond finger-level contact discrimination or broad grasping forces. Stimulations relating to innocuous pressure needed for grasping have been modulated to combine information regarding the sharpness of objects. The sharpness of objects was realized perceptually as varying levels of pain for the amputee subject. To provide these sensations at the phantom hand, neuromorphic spiking of the electrical signal is needed. By mimicking known spiking patterns of healthy afferent fibers in response to different stimuli, the amputee subject was also able to distinguish flat, rounded, and sharply pointed objects from one another based on the sharpness of the objects with high accuracy.<sup>47</sup>

Even with non-invasive, transcutaneous electrical stimulation techniques, potential complications can arise. Stimulation parameters (current, voltage, waveform) must be appropriately selected to reliably illicit sensation while minimizing spreading of the stimulation and preventing pain.<sup>46,47,67</sup> Electrode density must also be sufficient to stimulate the target region without activating nearby off-target neurons. Peripheral sensory and motor pathways in the residual limb need to be identified and distinguished well enough to deliver specific limb stimulation, particularly with myoelectric prostheses that use EMG to control grasping.<sup>67</sup> The task is further complicated by changes in the peripheral nervous systems due to original tissue damage followed by endogenous healing processes of the residual limb, as well as potential plasticity changes in the central nervous system from altered or absence of signaling.<sup>67</sup>

Strategies other than electrical stimulation have also been explored for sensory substitution strategies. Vibro-tactile stimulation methods use a haptic motor on the skin surface to provide vibrational sensation.<sup>10</sup> Similar to typical electrical sensory substitution, vibro-tactile stimulation is most effective when localized to the bicep region. Desensitization to prolonged stimulation is also a concern for vibro-tactile stimulation. After a minute of stimulation, subjects usually lose the ability to recognize the presence of vibrational stimulation. For linearly increasing vibration intensity with increasing grasping force, vibrotactile feedback is most useful at intermediate grasping forces. When minimal grasping force or full grip strength is needed, vibrational stimulation does not improve upon the intended grip strength.<sup>10</sup>

Since desensitization to prolonged vibro-tactile stimulation is of concern, the strategy of encoding for contact onset and release of objects can be more successful than encoding for prolonged contact. By using this event-driven approach for contact, picking up, setting down, and releasing an object, amputee subjects reported improved performance when grasping and manipulating fragile objects. Minimal training was needed, as most subjects reported grasping improvement within a week, while some showed improvement immediately upon introduction of the event-driven vibrotactile stimulation.<sup>17</sup> The design of the tested system, called the Discrete Event-driven Sensory feedback Control (DESC) system, was such that it could be used with an existing prosthesis. A flexible thimble with embedded sensors was placed over the forefinger and thumb and connected to two vibro-tactile stimulators located on the upper arm near the bicep of amputee subject. In grasping trials with a fragile block, the use of DESC feedback helped prevent subjects from breaking the boxes due to excessive compression ( $> 10$  N).<sup>17</sup>

Mechano-tactile sensory stimulation involves the use of physical pressure or tangential stretch mechanisms that resemble the sensation of applied force.<sup>2</sup> Passive, linear skin stretch methods use simple pulley systems attached to the prosthetic fingers and adhesive contact pads on the residual limb to directly translate finger flexion with a purely mechanical solution. Since finger positioning and hand aperture are being utilized, the subjects were provided with proprioceptive feedback rather than a direct grasping force. By using mechano-tactile stretch stimulation, subjects could reliably report stable configurations of the prosthetic thumb, index finger, and middle finger with 88% accuracy as well as move the prosthetic fingers into a target grip aperture with only 11% error.<sup>2</sup>

Mechano-tactile stimulation can also be expanded to include a localized contact force on the residual limb in addition to tangential shear stretching. The clenching upper-limb force feedback (CUFF) mechano-tactile device uses an elastic belt around the upper arm to induce pressure and stretch stimuli.<sup>9</sup> The normal force or pressure stimulation is applied around the entire circumference of the arm by tightening the band. Stretch stimulation is created by rotating the armband. Friction between the armband and skin provides a pulling effect. Three levels of object stiffness discrimination were achieved when relying on CUFF stimulation from a prosthetic hand grasping the target objects.<sup>9</sup>

Cable-driven and linear tactor systems have also been used to provide mechano-tactile stimulation.<sup>57</sup> In these systems, the tactor is a rounded bolt that is used to apply a normal force to the skin. Linear tactor

systems can be bulkier and more cumbersome for users. Cable-driven systems have a lower profile, but also take up more space along the length of the residual limb. When using two cable-driven tactors corresponding to the thumb and forefinger, proper discrimination of which respective prosthetic fingers were being stimulated was achieved. Additionally, the grasping force used in object manipulation tasks decreased, showing that subjects were better at recognizing the adequate grasping force needed.<sup>57</sup> Figure 6 shows the common extra-dermal stimulation strategies discussed.

Visual feedback is another avenue that has been explored for the potential of providing sensory stimulation in upper limb prostheses.<sup>18,42</sup> Visual feedback is more technologically complicated to develop, but is now more accessible with devices that have been designed for general use. Using an augmented reality display in the peripheral view, information regarding grasping force and prosthetic hand aperture is learned and incorporated by subjects in manipulation tasks.<sup>18</sup> The GLIMPSE system uses the Google Glass headband to relay information regarding EMG signals, hand aperture, force, and contact events with an augmented reality display in the user's peripheral vision.<sup>42</sup> The peripheral visual feedback presented allowed for more control in manipulation tasks that required accurate control of grasping forces.<sup>42</sup> This suggests that visual feedback is another viable sensory replacement strategy for improving upper-limb prosthesis control.

Using combinations of different sensory stimulation modalities is also possible. Vibration and electrical stimulation have been combined in the hybrid vibro-electro-tactile (HyVE) sensory feedback system.<sup>21</sup> Even when stimulated in parallel, subjects are able to independently discriminate electrical and vibrational stimulations. When testing user perception discrimination of nine different messages, which could be used for training subjects with sensory substitution, a combination of vibro-tactile and electro-tactile stimulation improved recognition accuracy to 72% from 29% and 44% for each individual stimulation modality, respectively.<sup>21</sup> This shows the possibility of increasing the number of sensory signals that can be distinguished without increasing the space needed on the skin surface. It may be most valuable to use vibration for event-driven signaling,<sup>17</sup> while also using electrical stimulation for grasping force or hand aperture.<sup>3,66,71</sup>

Extra-dermal sensory stimulation techniques are a viable, non-invasive solution to aid in grasping tasks with upper limb prostheses. Sensory substitution can be achieved by replacing lost limb sensations with alternative stimuli on the residual limb or other skin surfaces. Purely mechanical solutions can be used to



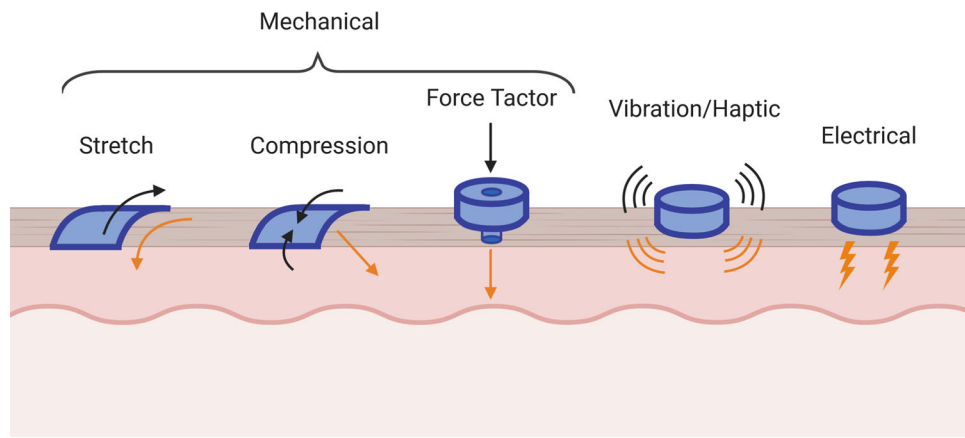


**FIGURE 6.** Visualization of extra-dermal stimulation strategies. Stretch and compression are applied using an armband wrapped around the circumference of the arm. The force tactor provides a more localized mechanical stimulation. Vibration and electrical stimulation are more common and can be readily sourced.

pull the skin surface and provide proprioceptive feedback regarding the prosthetic hand aperture. Haptic motor vibration and low-voltage surface electrode stimulation can be used to create sensory stimulation systems with lower profiles, but require onboard circuitry. Visual feedback with augmented reality displays in the peripheral vision can also improve object manipulation with prostheses. Transcutaneous electrical nerve stimulation (TENS) can be used to stimulate the phantom limb by targeting the median and ulnar nerves in the residual limb, thereby providing sensory feedback that is perceived to originate from the lost limb rather than directly on electrode contact site. Perhaps the greatest benefit of these techniques is that they require no surgery or recovery periods for prosthetic users; rather, these stimulation techniques can often be directly added to existing prostheses.

#### *Subdermal Stimulation*

Another method of interfacing with the peripheral nervous system to replace lost sensory stimulation is more direct, requiring subcutaneous implantation of specifically designed electrode systems.<sup>54,60,67</sup> There are varying levels of contact with the target nerves, the trade-off being the extent of how invasive the system is and the surgical procedure needed for implantation against the level of precision and specificity that the electrodes can achieve.<sup>60,67</sup> Strategies for interfacing with the central nervous system have also been studied, including those directly stimulating the brain and spinal cord.<sup>4</sup> Our review will focus on strategies for stimulating the peripheral nervous system that rely on intact neural pathways for signal propagation of sensory stimulation from the peripheral nervous system to the central nervous system for perception. Figure 7 shows examples of the most common and novel sub-

dermal electrode designs, highlighting their unique design characteristics.

One strategy for implanted electrodes is to surround the targeted peripheral nerve without breaking the outer layer of epineurium around the nerve, creating an extra-neural electrode (Fig. 7).<sup>61</sup> The non-penetrating, spiral nerve cuff electrode wraps around the nerve twice over.<sup>13</sup> This neural cuff electrode relies on a polymer sheath that is engineered to naturally curl into a cylindrical form. When curled, the electrodes align in a circular pattern, creating a cross-section of electrical stimulation perpendicular to the length of the nerve. The curling of the polymer sheath allows for the spiral nerve cuff electrode to be used with a range of nerve sizes, stretching around larger nerves while maintaining a secure fit. If there is considerable strain, the nerve cuff electrode can become dislodged from the nerve, avoiding damage but also resulting in electrode-nerve contact loss. Due to the extra-neural nature of the spiral nerve cuff electrode, it primarily targets fascicles near the epineurium of the nerve. In trans-radial amputee subjects, the spiral cuff electrode has been used to artificially stimulate tactile sensations in the peripheral limb, functionally allowing for the replacement of some somatosensory feedback in the lost limb.<sup>13</sup>

The flat interface nerve electrode (FINE) is another extra-neural electrode design that does not penetrate the epineurium.<sup>7,62</sup> The FINE design is similar to the spiral nerve electrodes, but it also imposes a mechanical clamping action that physically deforms the target nerve into a flatter cross-sectional area (Fig. 7). This clamping action creates an altered physical separation of the fascicles and decreases the distance from individual electrodes to the medial fascicles. Therefore, targeting individual fascicles, including those that are beyond the range of the spiral nerve cuff electrodes,

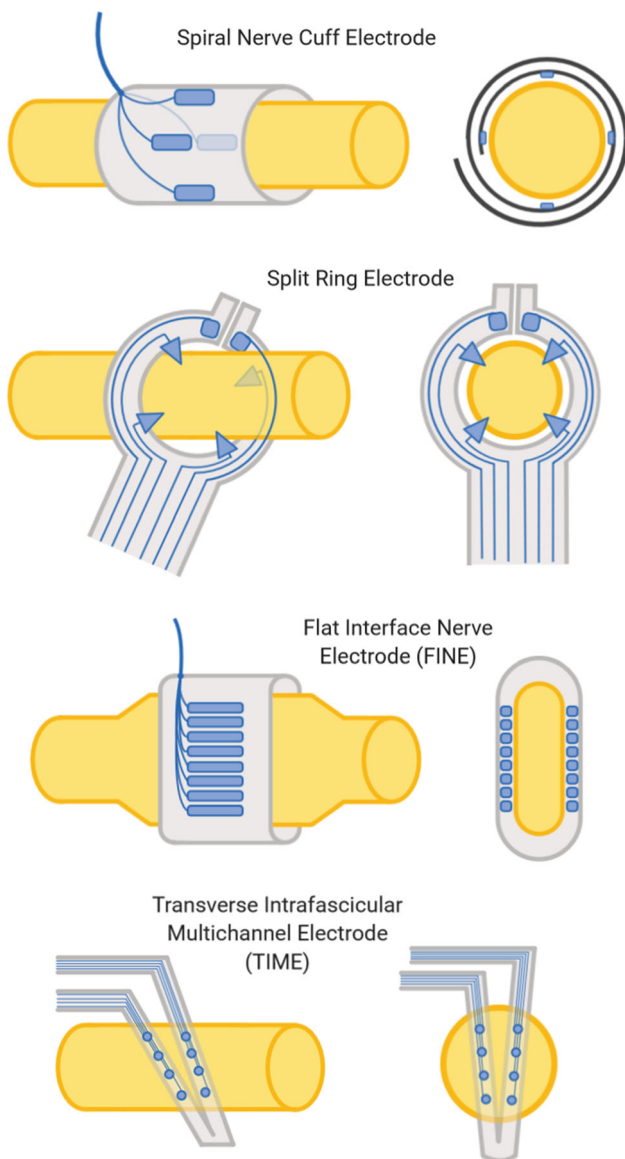


**FIGURE 7.** Intradermal electrode designs (Cuff, Flat Interface, Split Ring, and Transverse Intra-fascicular electrodes) showing active sites of the electrodes (blue) and afferent nerve (yellow) placement. Recruitment of different regions of neurons along the nerve can be inferred from the proximity to the active sites on the electrodes.

becomes possible.<sup>56</sup> Two 8-channel FINE cuffs implanted on the median and ulnar nerves, in conjunction with a 4-channel spiral nerve cuff electrode on the radial nerve, were used to restore phantom limb sensations of pressure, vibration, tapping, and rubbing in an amputee.<sup>62</sup>

Split ring electrodes, previously called c-shaped electrodes,<sup>72</sup> contact the epineurium layer with four protruding electrodes along the inner diameter of the nerve-surrounding ring<sup>34</sup> (Fig. 7). The electrode was fabricated with layered polyimides and Au/Pt active sites. The ring portion of the electrode is split at one

end, allowing for it to be spread apart for implantation around a nerve and also lending itself to minor deformation due to nerve displacement at each contact point. The split ring electrodes have been tested for stimulation and recording paradigms.

Intra-fascicular electrodes penetrate the epineurium and the perineurium to directly interface with the fascicles of the target nerves. The longitudinal intra-fascicular electrode (LIFE) consists of a single contact point at the end of a platinum-iridium wire or other flexible insulated wires.<sup>64</sup> The electrode is implanted into the fascicle with a rigid needle sheath that is then removed.

The distributed intra-fascicular multi-electrode (DIME) system was engineered by coiling multiple LIFEs into a silicone tube for implantation.<sup>64</sup> Once implanted, the distal active end of each LIFE is exposed by heating with a tungsten rod or narrow laser beam. The effective cross-section of electrode contact points can be varied by relocating the active site of each LIFE from the distal end to a more proximal location. Surgical implantation, peripheral motor nerve stimulation, and recording of the tibial fascicles have been tested. These studies used 6-electrode DIMEs that targeted medial and ulnar nerves. Functional stimulation was shown by ankle movements, while afferent recordings were accomplished by passive limb manipulation.

Another intra-fascicular approach to peripheral nerve interfacing is the transverse intra-fascicular multichannel electrode (TIME).<sup>6,40</sup> The design of the TIME consists of four active sites on each side of a V-bent, polyimide, thin-film electrode that are transversely implanted into the nerve to directly contact with the fascicles (Fig. 7). Stimulation of sciatic nerves in the rat model have been achieved with the TIME.

Emerging techniques have sought to add therapeutic effects to the nerve, in addition to signal transduction through stimulation. Intra-fascicular electrodes have been developed with the aim of repairing nerve damage at the vicinity of stimulation sites.<sup>24</sup> Additionally, studies have demonstrated differentiation and regeneration of neuronal and non-neuronal cells of the nervous system through electrical stimulation<sup>33</sup> and through static magnetic field stimulation.<sup>50</sup> These techniques have the potential to be incorporated with sensory stimulation electrodes for future improvement.

It is also possible that future stimulation techniques may not require implanted electrodes. Upconversion nanoparticles (UCNPs) have been used with low spatial dispersion to activate neurons transfected with light-sensitive ion channels.<sup>11</sup> The characteristic property of UCNPs is their ability to convert multiple low-energy incident photons into a higher energy photon. By transfecting neurons with light-sensitive ion chan-

nels, as is commonly done with optogenetic studies, the released high-energy photons of the UCNPs can be tuned to the wavelengths of the light-sensitive ion channels in transfected neurons. UCNPs have been widely adopted<sup>25,36,49</sup> in the forefront of academic research, but clinical applications would be further off in the future. The use of UCNPs would require clinical translation, particularly regarding the local transfection of neurons with light-sensitive ion channels and validation of the prolonged stability of the UCNPs.

## ACKNOWLEDGMENTS

The authors thank Robert Wright, MLS for his guidance and expertise with database searching in order to find relevant publications. We additionally recognize the contributions of Brice Lapin, Jack Wright, and Yiyuan Zhang in the preliminary literature search and data collection. Select illustrations for this article were created with Biorender.com following an academic licensing agreement.

## AUTHOR CONTRIBUTION

AA, AM, SS, HK, and KD contributed to the conception and design. AM, SS, HK, and KD performed literature search, data analysis and drafted the manuscript. XL provided critical revision of the work. AA supervised and reviewed this work.

## FUNDING

This study did not receive any external funding. This article was in part supported by the Start-Up Tier 1 grant # 21.4531.162640 (PI: A. ALL) and by the Faculty Seed Fund # 31.4531.179234 (PI: A. ALL) from Hong Kong Baptist University (HKBU), Hong Kong.

## CONFLICT OF INTEREST

All authors declare no conflict of interest and have nothing to disclose.

## REFERENCES

- <sup>1</sup>Abraira, V. E., and D. D. Ginty. the sensory neurons of touch. *Neuron* 79:618–639, 2013.
- <sup>2</sup>Akhtar, A., M. Nguyen, L. Wan, B. Boyce, P. Slade, and T. Bretl. Passive Mechanical Skin Stretch for Multiple Degree-of-Freedom Proprioception in a Hand Prosthesis, 2014.
- <sup>3</sup>Arakeri, T. J., B. A. Hasse, and A. J. Fuglevand. Object discrimination using electrotactile feedback. *J. Neural Eng.* 15:046007, 2018.
- <sup>4</sup>Bensmaia, S. J., and L. E. Miller. Restoring sensorimotor function through intracortical interfaces: progress and looming challenges. *Nat. Rev. Neurosci.* 15:313, 2014.
- <sup>5</sup>Biddiss, E. A., and T. T. Chau. Upper limb prosthesis use and abandonment: a survey of the last 25 years. *Prosthet. Orthot. Int.* 31:236–257, 2007.
- <sup>6</sup>Boretius, T., J. Badia, A. Pascual-Font, M. Schuettler, X. Navarro, K. Yoshida, and T. Stieglitz. A transverse intrafascicular multichannel electrode (TIME) to interface with the peripheral nerve. *Biosens. Bioelectron.* 26:62–69, 2010.
- <sup>7</sup>Brill, N. A., S. N. Naufel, K. Polasek, C. Ethier, J. Cheesborough, S. Agnew, L. E. Miller, and D. J. Tyler. Evaluation of high-density, multi-contact nerve cuffs for activation of grasp muscles in monkeys. *J. Neural Eng.* 15:036003, 2018.
- <sup>8</sup>Cao, Y., T. Li, Y. Gu, H. Luo, S. Wang, and T. Zhang. Fingerprint-inspired flexible tactile sensor for accurately discerning surface texture. *Small* 14:1703902, 2018.
- <sup>9</sup>Casini, S., M. Morvidoni, M. Bianchi, M. Catalano, G. Grioli, and A. Bicchi. Design and realization of the CUFF - clenching upper-limb force feedback wearable device for distributed mechano-tactile stimulation of normal and tangential skin forces. In: *2015 IEEE/RSJ International Conference on Intelligent Robots and Systems (IROS)*. 2015. <https://doi.org/10.1109/iros.2015.7353520>.
- <sup>10</sup>Chaubey, P., T. Rosenbaum-Chou, W. Daly, and D. Boone. Closed-loop vibratory haptic feedback in upper-limb prosthetic users. *J. Prosthet. Orthot.* 26:120–127, 2014.
- <sup>11</sup>Chen, S., A. Z. Weitemier, X. Zeng, L. He, X. Wang, Y. Tao, A. J. Y. Huang, Y. Hashimoto-dani, M. Kano, H. Iwasaki, L. K. Parajuli, S. Okabe, D. B. L. Teh, A. H. All, I. Tsutsui-Kimura, K. F. Tanaka, X. Liu, and T. J. McHugh. Near-infrared deep brain stimulation via upconversion nanoparticle-mediated optogenetics. *Science* 359:679–684, 2018.
- <sup>12</sup>Chortos, A., J. Liu, and Z. Bao. Pursuing prosthetic electronic skin. *Nat. Mater.* 15:937–950, 2016.
- <sup>13</sup>Christie, B. P., M. Freeberg, W. D. Memberg, G. J. C. Pinault, H. A. Hoyen, D. J. Tyler, and R. J. Triolo. Long-term stability of stimulating spiral nerve cuff electrodes on human peripheral nerves. *J. NeuroEng. Rehabil.* 14:70, 2017.
- <sup>14</sup>Chun, S., A. Hong, Y. Choi, C. Ha, and W. Park. A tactile sensor using a conductive graphene-sponge composite. *Nanoscale* 8:9185–9192, 2016.
- <sup>15</sup>Chun, S., Y. Kim, H.-S. Oh, G. Bae, and W. Park. A highly sensitive pressure sensor using a double-layered graphene structure for tactile sensing. *Nanoscale* 7:11652–11659, 2015.
- <sup>16</sup>Chun, K.-Y., Y. J. Son, E.-S. Jeon, S. Lee, and C.-S. Han. A self-powered sensor mimicking slow- and fast-adapting cutaneous mechanoreceptors. *Adv. Mater.* 30:1706299, 2018.
- <sup>17</sup>Clemente, F., M. D'Alonzo, M. Controzzi, B. B. Edin, and C. Cipriani. Non-invasive, temporally discrete feedback of object contact and release improves grasp control of closed-loop myoelectric transradial prostheses. *IEEE Trans. Neural Syst. Rehabil. Eng.* 24:1314–1322, 2016.
- <sup>18</sup>Clemente, F., S. Dosen, L. Lonini, M. Markovic, D. Farina, and C. Cipriani. Humans can integrate augmented



- reality feedback in their sensorimotor control of a robotic hand. *IEEE Trans. Hum. Mach. Syst.* 47:583–589, 2017.
- <sup>19</sup>Cula, O. G., and K. J. Dana. Recognition methods for 3D textured surfaces. *Proc. SPIE* 2001. <https://doi.org/10.1117/12.429492>.
  - <sup>20</sup>Dahiya, R. S., G. Metta, M. Valle, and G. Sandini. Tactile sensing-from humans to humanoids. *TRO* 26:1–20, 2010.
  - <sup>21</sup>Dalonzo, M., S. Dosen, C. Cipriani, and D. Farina. HyVE: hybrid vibro-electrotactile stimulation for sensory feedback and substitution in rehabilitation. *IEEE Trans. Neural Syst. Rehabil. Eng.* 22:290–301, 2014.
  - <sup>22</sup>de Boissieu, F., C. Godin, B. Guilhamat, D. David, C. Serviere, D. Baudois. Tactile texture recognition with a 3-axial force MEMS integrated artificial finger, 2009. <http://doi.org/10.15607/rss.2009.v.007>.
  - <sup>23</sup>Ehrsson, H. H., B. Rosen, A. Stocksli, C. Ragnö, P. Kohler, and G. Lundborg. Upper limb amputees can be induced to experience a rubber hand as their own. *Brain* 131:3443–3452, 2008.
  - <sup>24</sup>FitzGerald, J. J., N. Lago, S. Benmerah, J. Serra, C. P. Watling, R. E. Cameron, E. Tarte, S. P. Lacour, S. B. McMahon, and J. W. Fawcett. A regenerative microchannel neural interface for recording from and stimulating peripheral axons in vivo. *J. Neural Eng.* 9:016010, 2012.
  - <sup>25</sup>Han, S., A. Samanta, X. Xie, L. Huang, J. Peng, S. J. Park, D. B. L. Teh, Y. Choi, Y.-T. Chang, A. H. All, Y. Yang, B. Xing, and X. Liu. Gold and hairpin DNA functionalization of upconversion nanocrystals for imaging and in vivo drug delivery. *Adv. Mater.* 29:1700244, 2017.
  - <sup>26</sup>Jamali, N., and C. Sammut. Majority voting: material classification by tactile sensing using surface texture. *IEEE Trans. Rob.* 27:508–521, 2011.
  - <sup>27</sup>Ji, Z., H. Zhu, H. Liu, N. Liu, T. Chen, Z. Yang, and L. Sun. The design and characterization of a flexible tactile sensing array for robot skin. *Sensors (Basel, Switzerland)* 16:201, 2016.
  - <sup>28</sup>Karim, S. A. A., M. H. Kamarudin, B. A. Karim, M. K. Hasan, and J. Sulaiman. Wavelet transform and fast fourier transform for signal compression: a comparative study. *J. IFET* 2011. <https://doi.org/10.1109/icedsa.2011.5959031>.
  - <sup>29</sup>Kim, D.-H., J.-H. Ahn, W. M. Choi, H.-S. Kim, T.-H. Kim, J. Song, Y. Y. Huang, Z. Liu, C. Lu, and J. A. Rogers. Stretchable and foldable silicon integrated circuits. *Science* 320:507–511, 2008.
  - <sup>30</sup>Kim, S.-H., J. Engel, C. Liu, and D. L. Jones. Texture classification using a polymer-based MEMS tactile sensor. *J. Micromech. Microeng.* 15:912–920, 2005.
  - <sup>31</sup>Kim, J., M. Lee, H. J. Shim, R. Ghaffari, H. R. Cho, D. Son, Y. H. Jung, M. Soh, C. Choi, S. Jung, K. Chu, D. Jeon, S.-T. Lee, J. H. Kim, S. H. Choi, T. Hyeon, and D.-H. Kim. Stretchable silicon nanoribbon electronics for skin prosthesis. *Nat. Commun.* 5:5747, 2014.
  - <sup>32</sup>Lamport, Z. A., H. F. Haneef, S. Anand, M. Waldrip, and O. D. Jurchescu. Tutorial: organic field-effect transistors: materials, structure and operation. *J. Appl. Phys.* 124:071101, 2018.
  - <sup>33</sup>Lee, H. U., A. Blasiak, D. R. Agrawal, D. T. B. Loong, N. V. Thakor, A. H. All, J. S. Ho, and I. H. Yang. Subcellular electrical stimulation of neurons enhances the myelination of axons by oligodendrocytes. *PLoS ONE* 12:e0179642, 2017.
  - <sup>34</sup>Lee, S., S. Sheshadri, Z. Xiang, I. Delgado-Martinez, N. Xue, T. Sun, N. V. Thakor, S.-C. Yen, and C. Lee. Selective stimulation and neural recording on peripheral nerves using flexible split ring electrodes. *Sens. Actuators B Chem.* 242:1165–1170, 2017.
  - <sup>35</sup>Liao, Z., W. Liu, Y. Wu, C. Zhang, Y. Zhang, X. Wang, and X. Li. A tactile sensor translating texture and sliding motion information into electrical pulses. *Nanoscale* 7:10801–10806, 2015.
  - <sup>36</sup>Liu, X., Y. Wang, X. Li, Z. Yi, R. Deng, L. Liang, X. Xie, D. T. B. Loong, S. Song, D. Fan, A. H. All, H. Zhang, L. Huang, and X. Liu. Binary temporal upconversion codes of  $Mn^{2+}$ -activated nanoparticles for multilevel anti-counterfeiting. *Nat. Commun.* 8:1–7, 2017.
  - <sup>37</sup>Llado, X., M. Petrou, and J. Marti. Surface texture recognition by surface rendering. *Optic Eng.* 2005. <https://doi.org/10.1117/1.1869994>.
  - <sup>38</sup>Lu, N., C. Lu, S. Yang, and J. Rogers. Highly sensitive skin-mountable strain gauges based entirely on elastomers. *Adv. Funct. Mater.* 22:4044–4050, 2012.
  - <sup>39</sup>Lucarotti, C., C. M. Oddo, N. Vitiello, and M. C. Carrozza. Synthetic and bio-artificial tactile sensing: a review. *Sensors (Basel, Switzerland)* 13:1435–1466, 2013.
  - <sup>40</sup>Maciejasz, P., J. Badia, T. Boretius, D. Andreu, T. Stieglitz, W. Jensen, X. Navarro, and D. Guiraud. Delaying discharge after the stimulus significantly decreases muscle activation thresholds with small impact on the selectivity: an in vivo study using TIME. *Med. Biol. Eng. Compu.* 53:371–379, 2015.
  - <sup>41</sup>Mannsfeld, S. C. B., B. C.-K. Tee, R. M. Stoltenberg, C. V. H.-H. Chen, S. Barman, B. V. O. Muir, A. N. Sokolov, C. Reese, and Z. Bao. Highly sensitive flexible pressure sensors with microstructured rubber dielectric layers. *Nat. Mater.* 9:859–864, 2010.
  - <sup>42</sup>Markovic, M., H. Karnal, B. Graimann, D. Farina, and S. Dosen. GLIMPSE: Google Glass interface for sensory feedback in myoelectric hand prostheses. *J. Neural Eng.* 14:036007, 2017.
  - <sup>43</sup>Muhammad, H. B., C. M. Oddo, L. Beccai, C. Recchiuto, C. J. Anthony, M. J. Adams, M. C. Carrozza, D. W. L. Hukins, and M. C. L. Ward. Development of a bioinspired MEMS based capacitive tactile sensor for a robotic finger. *Sens. Actuators A* 165:221–229, 2011.
  - <sup>44</sup>Muhammad, H. B., C. Recchiuto, C. M. Oddo, L. Beccai, C. J. Anthony, M. J. Adams, M. C. Carrozza, and M. C. L. Ward. A capacitive tactile sensor array for surface texture discrimination. *Microelectron. Eng.* 88:1811–1813, 2011.
  - <sup>45</sup>Nicolò, B., and B-B Gabriel. Effects of Chai3D Texture Rendering Parameters on Texture Perception, 2018. <http://doi.org/10.5281/zenodo.1287011>.
  - <sup>46</sup>Oddo, C. M., S. Raspopovic, F. Artoni, A. Mazzoni, G. Spigler, F. Petrini, F. Giambattistelli, F. Vecchio, F. Miraglia, L. Zollo, G. Di Pino, D. Camboni, M. C. Carrozza, E. Guglielmelli, P. M. Rossini, U. Faraguna, and S. Micera. Intraneural stimulation elicits discrimination of textural features by artificial fingertip in intact and amputee humans. *eLife* 5:e09148, 2016.
  - <sup>47</sup>Osborn, L. E., A. Dragomir, J. L. Betthausen, C. L. Hunt, H. H. Nguyen, R. R. Kaliki, and N. V. Thakor. Prosthesis with neuromorphic multilayered e-skin perceives touch and pain. *Sci. Rob.* 3:eaat3818, 2018.
  - <sup>48</sup>Pang, C., G.-Y. Lee, T. Kim, S. M. Kim, H. N. Kim, S.-H. Ahn, and K.-Y. Suh. A flexible and highly sensitive strain-gauge sensor using reversible interlocking of nanofibres. *Nat. Mater.* 11:795–801, 2012.
  - <sup>49</sup>Peng, J., A. Samanta, X. Zeng, S. Han, L. Wang, D. Su, D. T. B. Loong, N.-Y. Kang, S.-J. Park, A. H. All, W. Jiang, L. Yuan, X. Liu, and Y.-T. Chang. Real-time in vivo



- hepatotoxicity monitoring through chromophore-conjugated photon-upconverting nanoprobe. *Angew. Chem. Int. Ed.* 56:4165–4169, 2017.
- <sup>50</sup>Prasad, A., D. B. L. Teh, A. Blasiak, C. Chai, Y. Wu, P. M. Gharibani, I. H. Yang, T. T. Phan, K. L. Lim, H. Yang, X. Liu, and A. H. All. Static magnetic field stimulation enhances oligodendrocyte differentiation and secretion of neurotrophic factors. *Sci Rep.* 7:1–12, 2017.
  - <sup>51</sup>Qin, L., Z. Yi, and Y. Zhang. Enhanced surface roughness discrimination with optimized features from bio-inspired tactile sensor. *Sens. Actuators A* 2017. <https://doi.org/10.1016/j.sna.2017.07.054>.
  - <sup>52</sup>Qin, L., and Y. Zhang. Roughness discrimination with bio-inspired tactile sensor manually sliding on polished surfaces. *Sens. Actuators A* 279:433–441, 2018.
  - <sup>53</sup>Resnik, L., M. R. Meucci, S. Lieberman-Klinger, C. Fantini, D. L. Kelty, R. Disla, and N. Sasson. Advanced upper limb prosthetic devices: implications for upper limb prosthetic rehabilitation. *Arch. Phys. Med. Rehabil.* 93:710–717, 2012.
  - <sup>54</sup>Rijnbeek, E. H., N. Eleveld, and W. Olthuis. Update on peripheral nerve electrodes for closed-loop neuroprosthetics. *Frontiers Neurosci.* 2018. <https://doi.org/10.3389/fnins.2018.00350>.
  - <sup>55</sup>Ryu, S., P. Lee, J. B. Chou, R. Xu, R. Zhao, A. J. Hart, and S.-G. Kim. Extremely elastic wearable carbon nanotube fiber strain sensor for monitoring of human motion. *ACS Nano* 9:5929–5936, 2015.
  - <sup>56</sup>Schiefer, M. A., M. Freeberg, G. J. C. Pinault, J. Anderson, H. Hoyen, D. J. Tyler, and R. J. Triolo. Selective activation of the human tibial and common peroneal nerves with a flat interface nerve electrode. *J. Neural Eng.* 10:056006, 2013.
  - <sup>57</sup>Schoepp, K. R., M. R. Dawson, J. S. Schofield, J. P. Carey, and J. S. Hebert. Design and integration of an inexpensive wearable mechanotactile feedback system for myoelectric prostheses. *J. IEEE Transl. Eng. Health Med.* 2018. <http://doi.org/10.1109/jtehm.2018.2866105>.
  - <sup>58</sup>Shin, H., Z. Watkins, H. Huang, Y. Zhu, and X. Hu. Evoked haptic sensations in the hand via non-invasive proximal nerve stimulation. *J. Neural Eng.* 15:046005, 2018.
  - <sup>59</sup>Song, A., Y. Han, H. Hu, and J. Li. A novel texture sensor for fabric texture measurement and classification. *IEEE Trans. Instrum. Meas.* 63:1739–1747, 2014.
  - <sup>60</sup>Svensson, P., U. Wijk, A. Björkman, and C. Antfolk. A review of invasive and non-invasive sensory feedback in upper limb prostheses. *Expert Rev. Med. Dev.* 14:439–447, 2017.
  - <sup>61</sup>Tan, D. W., M. A. Schiefer, M. W. Keith, J. R. Anderson, and D. J. Tyler. Stability and selectivity of a chronic, multi-contact cuff electrode for sensory stimulation in human amputees. *J. Neural Eng.* 12:026002, 2015.
  - <sup>62</sup>Tan, D. W., M. A. Schiefer, M. W. Keith, J. R. Anderson, J. Tyler, and D. J. Tyler. A neural interface provides long-term stable natural touch perception. *Sci. Transl. Med.* 6:257, 2014.
  - <sup>63</sup>Tee, B. C.-K., A. Chortos, A. Berndt, A. K. Nguyen, A. Tom, A. McGuire, Z. C. Lin, K. Tien, W.-G. Bae, H. Wang, P. Mei, H.-H. Chou, B. Cui, K. Deisseroth, T. N. Ng, and Z. Bao. A skin-inspired organic digital mechanoreceptor. *Science* 350:313–316, 2015.
  - <sup>64</sup>Thota, A. K., S. Kuntaegowdanahalli, A. K. Starosciak, J. J. Abbas, J. Orbay, K. W. Horch, and R. Jung. A system and method to interface with multiple groups of axons in several fascicles of peripheral nerves. *J. Neurosci. Methods* 244:78–84, 2015.
  - <sup>65</sup>Tiwana, M. I., S. J. Redmond, and N. H. Lovell. A review of tactile sensing technologies with applications in biomedical engineering. *Sens. Actuators A* 179:17–31, 2012.
  - <sup>66</sup>Trbac, M., M. Beli, M. Isakovi, V. Koji, G. Bijeli, I. Popovi, M. Radoti, S. Doen, M. Markovi, D. Farina, and T. Keller. Integrated and flexible multichannel interface for electrotactile stimulation. *J. Neural Eng.* 13:046014, 2016.
  - <sup>67</sup>Tyler, D. J. Neural interfaces for somatosensory feedback: bringing life to a prosthesis. *Curr. Opin. Neurol.* 28:574–581, 2015.
  - <sup>68</sup>Volkmar, R., S. Dosen, J. Gonzalez-Vargas, M. Baum, and M. Markovic. Improving bimanual interaction with a prosthesis using semi-autonomous control. *J. NeuroEng. Rehabil.* 16:140, 2019.
  - <sup>69</sup>Wettels, N., V. J. Santos, R. S. Johansson, and G. E. Loeb. Biomimetic tactile sensor array. *Adv. Rob.* 22:829–849, 2008.
  - <sup>70</sup>Wu, Y., Y. Liu, Y. Zhou, Q. Man, C. Hu, W. Asghar, F. Li, Z. Yu, J. Shang, G. Liu, M. Liao, and R.-W. Li. A skin-inspired tactile sensor for smart prosthetics. *Sci. Rob.* 2018. <https://doi.org/10.1126/scirobotics.aat0429>.
  - <sup>71</sup>Xu, H., D. Zhang, J. C. Huegel, W. Xu, and X. Zhu. Effects of different tactile feedback on myoelectric closed-loop control for grasping based on electrotactile stimulation. *IEEE Trans. Neural Syst. Rehabil. Eng.* 24:827–836, 2016.
  - <sup>72</sup>Xue, N., T. Sun, W. M. Tsang, I. Delgado-Martinez, S.-H. Lee, S. Sheshadri, Z. Xiang, S. Merugu, Y. Gu, S.-C. Yen, and N. V. Thakor. Polymeric C-shaped cuff electrode for recording of peripheral nerve signal. *Sens. Actuators B Chem.* 210:640–648, 2015.
  - <sup>73</sup>Yeo, J. C., Z. Liu, Z. Zhang, P. Zhang, Z. Wang, and C. T. Lim. Wearable mechanotransduced tactile sensor for haptic perception. *Adv. Mater. Technol.* 2:1700006, 2017.
  - <sup>74</sup>Yi, Z., and Y. Zhang. Bio-inspired tactile FA-I spiking generation under sinusoidal stimuli. *J. Bionic Eng.* 13:612–621, 2016.
  - <sup>75</sup>Yi, Z., Y. Zhang, and J. Peters. Bioinspired tactile sensor for surface roughness discrimination. *Sens. Actuators A* 2017. <https://doi.org/10.1016/j.sna.2016.12.021>.
  - <sup>76</sup>Yousef, H., M. Boukallel, and K. Althoefer. Tactile sensing for dexterous in-hand manipulation in robotics—a review. *Sens. Actuators A* 167:171–187, 2011.
  - <sup>77</sup>Zhang, T., L. Jiang, and H. Liu. Design and functional evaluation of a dexterous myoelectric hand prosthesis with biomimetic tactile sensor. *IEEE Trans. Neural Syst. Rehabil. Eng.* 26:1391–1399, 2018.
  - <sup>78</sup>Zhao, H., K. O'Brien, S. Li, and R. F. Shepherd. Optoelectronically innervated soft prosthetic hand via stretchable optical waveguides. *Sci. Rob.* 1:eaa17529, 2016.
  - <sup>79</sup>Zhu, G., W. Q. Yang, T. Zhang, Q. Jing, J. Chen, Y. S. Zhou, P. Bai, and Z. L. Wang. Self-powered, ultrasensitive, flexible tactile sensors based on contact electrification. *Nano Lett.* 14:3208, 2014.
  - <sup>80</sup>Zollo, L., G. Di Pino, A. L. Ciancio, F. Ranieri, F. Cordella, C. Gentile, E. Noce, R. A. Romeo, A. D. Bellingegni, G. Vadalà, S. Miccinilli, A. Mioli, L. Diaz-Balzani, M. Bravi, K.-P. Hoffmann, A. Schneider, L. Denaro, A. Davalli, E. Gruppioni, R. Sacchetti, S. Castellano, V. Di Lazzaro, S. Sterzi, V. Denaro, and E. Guglielmelli. Restoring tactile sensations via neural interfaces for real-time force-and-slippage closed-loop control of bionic hands. *Sci. Rob.* 4:e9924, 2019.

- <sup>81</sup>Zou, L., C. Ge, Z. J. Wang, E. Cretu, and X. Li. Novel tactile sensor technology and smart tactile sensing systems: a review. *Sensors* 17:2653, 2017.
- <sup>82</sup>Zou, Z., C. Zhu, Y. Li, X. Lei, W. Zhang, and J. Xiao. Rehealable, fully recyclable, and malleable electronic skin enabled by dynamic covalent thermoset nanocomposite. *Sci. Adv.* 4:eaag0508, 2018.

**Publisher's Note** Springer Nature remains neutral with regard to jurisdictional claims in published maps and institutional affiliations.